Dalton Transactions

ROYAL SOCIETY OF CHEMISTRY

PAPER

View Article Online
View Journal | View Issue

Cite this: *Dalton Trans.*, 2022, **51**, 16508

Structural principles of cation ordering and octahedral tilting in A-site ordered double perovskites: ferroelectric $CaMnTi_2O_6$ as a model system†

Elisabeth K. Albrecht and Antti J. Karttunen *

Received 14th July 2022,
Accepted 12th October 2022

DOI: 10.1039/d2dt02283d

rsc.li/dalton

We have used quantum chemical methods to study the structural principles and energetics of A-site ordered $AA'B_2O_6$ double perovskites. 33 combinations of A-site ordering and Glazer tilting have been systematically studied for the ferroelectric $CaMnTi_2O_6$ model system. The used approach was able to predict the correct combination of A-site ordering and tilting of octahedra in comparison to the experimentally known $CaMnTi_2O_6$. The energy differences between the various combinations of A-site ordering and tilt systems show a large variation of tens of kJ mol^{-1} per formula unit, which suggests that the methodology used here can be used as a starting point for making reliable predictions on the structures of yet unknown A-site ordered double perovskites. The energy differences due to A-site ordering and octahedral tilting were larger compared to the energy difference arising from ferroelectric distortion in $CaMnTi_2O_6$. The energy differences between various hypothetical double perovskite structures could be explained by studying their structural characteristics in detail. The relative energies are closely correlated with the Mn–O distances and Mn coordination in the studied structures.

1 Introduction

Perovskites are a broad class of compounds showing a large variety of technologically relevant functionalities such as piezoelectricity, pyroelectricity, ferroelectricity, multiferroicity, and superconductivity.[1] In the basic perovskite structure with the general structural formula ABX_3 (space group $Pm\bar{3}m$), twelve-coordinated A cations are located at the corners of the primitive cubic unit cell, while the B cations are octahedrally coordinated by X anions located on the face centers of the unit cell. The anion octahedra are corner-linked. The most common anion is oxygen, leading to oxide perovskites ABO_3, but other elements such as fluorine and chlorine can also be found at the X-site. By tuning the relative sizes and oxidation states of the cations and anions, the physical properties of perovskite materials can be modified and adapted to different requirements.[1–3]

Most perovskite materials do not exhibit the perfect, ideal crystal structure in the space group $Pm\bar{3}m$. For example, a size mismatch of the cations can lead to the tilting of the BX_6 octahedra or electronic effects can result in the distortion of the BX_6 octahedra.[4] Glazer proposed the most common notation for the tilting of octahedra in perovskites in his 1972 paper.[5] In the Glazer notation, *a*, *b*, and *c* stand for the pseudocubic unit cell parameters in the three crystallographic directions. The pseudocubic unit cell, compared to the real unit cell, always refers to the cell around exactly one octahedron. If the octahedral tilts about two axes and therefore the lattice parameters in these directions are the same, they are described with the same letter. For example, in notation *aac*, the first two lattice parameters would be the same and the third would be different. Due to their linked corners, the rotation of one octahedron about a pseudocubic axis determines the rotations of all octahedra in the same plane. Along one axis, the octahedra can all be rotated in line, alternating, or not at all. These rotations are denoted by superscripts +, −, and 0, respectively. For example, notation $a^+a^+c^0$ means that the pseudocubic lattice parameters are the same in the *a* and *b* directions, but different in the *c* direction, while the octahedra are tilted in line about the *a* and *b* axes but are not tilted about the *c* axis. Fig. 1 shows an ideal, untilted perovskite structure and two examples of perovskite structures with tilted octahedra. For a more detailed explanation of the Glazer notation and its symmetry relations, see the articles by Glazer[5] and Woodward.[6,7]

Department of Chemistry and Materials Science, Aalto University, P.O. Box 16100, FI-00076 Aalto, Finland. E-mail: antti.karttunen@aalto.fi

†Electronic supplementary information (ESI) available: Crystal structures of the studied double perovskite systems in CIF format, the absolute electronic energies of the studied systems, and additional computational details. See DOI: https://doi.org/10.1039/d2dt02283d

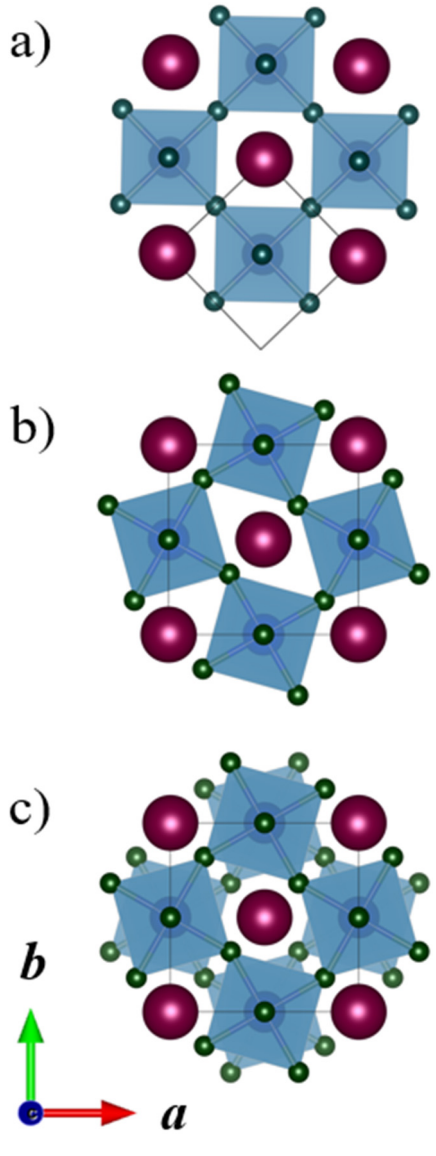

Fig. 1 Perovskites with different Glazer tilt systems along the *c* direction: (a) ideal, untilted, (b) $a^0a^0c^+$, and (c) $a^0a^0c^-$. The A-site cations are in dark red, the B-site cations and their coordination polyhedra in blue, and the X-site anions in green. The unit cell in each system is drawn in black. All crystal structure illustrations in the manuscript have been prepared with the VESTA program.[8]

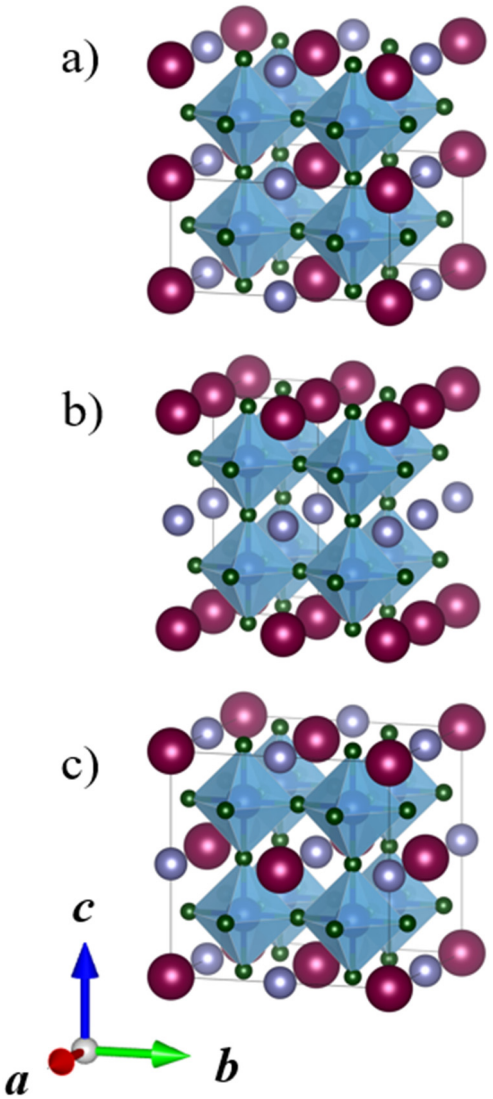

Fig. 2 A-site ordered double perovskites with (a) columnar, (b) planar, and (c) rock salt ordering. The two cation species on the A-site are shown in dark red and purple, the B-site cations and their coordination polyhedra in blue, and the X-site anions in green. The unit cell in each system is drawn in black.

Perovskites, where the A sites or B sites are occupied with two different cations ordering in a certain way are called double perovskites.[1,9,10] A-site ordered double perovskites with the general formula $AA'B_2X_6$ have two different cations on the A-site, while B-site ordered double perovskites with the general formula $A_2BB'X_6$ have two different cations on the B-site. Three different orderings of the cations are typically considered: columnar, planar, and rock-salt. Fig. 2 illustrates these orderings for A-site ordered double perovskites. Columnar, one-dimensional ordering, means that the cations of one type (A) form columns in one direction and these columns are surrounded by columns of the other cation type (A′). In planar, two-dimensional ordering, planes of A and A′ cations are alternating. The rock-salt ordering is a three-dimensional ordering, where each A cation has only A′ cations as the nearest neighbours. While A-site ordered double perovskites are often in the planar ordering, in B-site ordered double perovskites the rock salt ordering is the most common one.[9,11–13] A-site cation ordering is much less common than B-site cation ordering and in the majority of the known $AA'B_2X_6$ perovskites, the A and A′ cations do not order. The general principles of cation ordering in both A-site and B-site ordered double perovskites have been discussed in detail by King and Woodward.[9]

Various possibilities for cation ordering and octahedral tilting lead to a large number of structural varieties in the case of double perovskites, as illustrated by a systematic survey on

B-site ordered $A_2BB'O_6$ double perovskites.[13] This also complicates the efforts to predict the crystal structures of novel double perovskites just based on their elemental composition. Such predictive approaches would also be helpful when determining the exact crystal structure of newly synthesized double perovskite materials by powder X-ray diffraction, as the diffraction patterns of different structural alternatives may sometimes be too similar to confidently be distinguished. In fact, often after determining secondary properties, the cation ordering or octahedral tilting pattern can be deduced.

In the case of simple ABX_3 perovskites, Goldschmidt proposed already in 1926 a simple expression for tolerance factor t that could be used to predict the crystal system of a perovskite based on the ionic radii of A, B, and X.[14] The simple Goldschmidt tolerance does not take octahedral tilting into account in any way, nor does it offer any insight into the ordering of the cations in double perovskites. Despite this, it is still useful as a starting point in high-throughput screening studies for predicting potential perovskite compositions, where additional geometric criteria for octahedral tilting have been included.[15] New tolerance factor τ, incorporating the oxidation states of the cations, has also been derived for $A_2BB'X_6$ double perovskites, and stability rankings of potential new double perovskites have been derived based on it.[16] Similar to the original tolerance factor formula, the τ formula does not take octahedral tilting into account, nor does it offer any insights into the ordering of the cations.

Compared to structure prediction approaches based on geometric parameters such as ionic radii, quantum chemical calculations with Density Functional Theory (DFT) provide computationally more intensive, but at the same time, much more powerful structure prediction approaches. DFT methods can assess the relative stability of any existing or predicted perovskite structure, taking fully into account all structural variations such as cation ordering, tilting of octahedra, and displacement of A- or B-site cations. A recent example of the use of DFT methods is in the report of Shojaei and Yin, where they studied ABX_3 perovskite halides (A = Cs, Rb, K; B = Pb, Sn; X = I, Br, Cl) to correlate their energetics and octahedral tilting energies with known stability descriptors of perovskite halides.[17] Also, Ding *et al.* compared few different tilt systems for the B-site ordered double perovskite Sr_2CoRuO_6 to confirm its cation ordering.[18] However, to our knowledge, systematic DFT studies have not been used to create stability rankings of A-site or B-site ordered double perovskites with different octahedral tilt patterns.

Here, we present a quantum chemical investigation of cation ordering and octahedra tilting in A-site ordered $AA'B_2O_6$ double perovskites. We systematically study all relevant combinations of cation ordering and tilting of octahedra to provide a solid foundation for structure prediction and structure elucidation of A-site ordered $AA'B_2O_6$ double perovskites with DFT methods. At the same time, we study in detail the energetic effects of structural variations for several known $AA'B_2O_6$ double perovskites. As our main benchmark system, we used $CaMnTi_2O_6$ which is a ferroelectric A-site ordered double perovskite oxide with potential piezoelectric and pyroelectric properties. It is also being investigated as a Pb- and Bi-free photovoltaic material.[19–22] The ferroelectricity of $CaMnTi_2O_6$ also provides insight into the energetic effects of structural distortion beyond the tilting of the octahedra.

2 Procedure and methods

2.1 Tilt systems and cation ordering

To study the different combinations of the A-site cation ordering and octahedral tilt system for $CaMnTi_2O_6$, suitable tilt systems were first selected. Glazer described 23 tilt systems in his original paper,[5] but after a group theoretical analysis,[23] 15 simple distinct tilt systems remained. Out of these 15 tilt systems, 11 were taken into account for this work, as the remaining four tilt systems are low symmetry/transitional tilt systems that are observed as intermediates in a phase transition between higher symmetry structures.[24] These 11 tilt systems are listed in Table 1 and they are in line with the current version of the SPuDS software that includes one additional tilt system in comparison to the original SPuDS paper.[24]

For each space group and tilt system, experimentally known perovskite crystal structures were searched from the structural databases and literature, and if an existing structure was available, then it was used to create the corresponding $CaMnTi_2O_6$ double perovskite structure template with columnar, planar, or rock salt ordering. If there was no existing perovskite crystal structure available for a certain tilt system, then the structure was built manually using the VESTA software.[8] The tilt system $a^-a^-a^-$ (space group $R\bar{3}c$) produced hexagonal unit cells. For the sake of comparability, calculations have been done with a pseudo-tetragonal (columnar, planar) or pseudo-cubic (rock salt) unit cell. These were obtained by deriving a unit cell with antiferromagnetic (AFM) ordering of the magnetic Mn(II) ions. For other tilt systems, the majority of the calculations were carried out for a ferromagnetic (FM) ground state, as there is no significant magnetic coupling between the Mn(II) ions. We found the FM and AFM ground states to show energy differences of less than 1 kJ mol^{-1}. This finding is in line with the

Table 1 Glazer tilt systems taken into account in this work. The tilt number refers to the number given by Glazer[5]

	Tilt class	Tilts	Tilt number	Space group
Zero-tilt	000	$a^0a^0a^0$	23	$Pm\bar{3}m$ (221)
One-tilt	00−	$a^0a^0c^-$	22	$I4/mcm$ (140)
	00+	$a^0a^0c^+$	21	$P4/mbm$ (127)
Two-tilt	0−−	$a^0b^-b^-$	20	$Imma$ (74)
	+0−	$a^+b^0c^-$	17	$Cmcm$ (63)
	0++	$a^0b^+b^+$	16	$I4/mmm$ (139)
Three-tilt	−−−	$a^-a^-a^-$	14	$R\bar{3}c$ (167)
		$a^-b^-b^-$	13	$C2/c$ (15)
	−+−	$a^-b^+a^-$	10	$Pnma$ (62)
	++−	$a^+a^+c^-$	5	$P4_2/nmc$ (137)
	+++	$a^+a^+a^+$	3	$Im\bar{3}$ (204)

results of Gou *et al.*, who studied the different spin configurations of $CaMnTi_2O_6$ with the HSE06 hybrid density functional method.[19] For a few systems, the AFM ground state was used for purely technical reasons, to avoid convergence issues of the self-consistent field procedure during the DFT calculations (columnar $a^0b^+b^+$ and $a^0a^0c^-$ tilt systems, planar $a^-b^-b^-$, $a^0a^0c^+$, and $a^0a^0c^-$ tilt systems, and rock salt $a^0b^+b^+$ tilt system).

In addition to the hypothetical $CaMnTi_2O_6$ double perovskite structures described above, we included the experimentally determined crystal structure of $CaMnTi_2O_6$ in order to compare the theoretical results with the experimental results. The magnetic, electronic, and dielectric properties of the experimentally determined crystal structure were thoroughly studied by Gou *et al.*[19]

2.2 Computational details

The CRYSTAL17[25] program package was used for all quantum chemical calculations. The hybrid PBE0 density functional method, (DFT-PBE0),[26,27] was used in combination with all-electron, Gaussian-type basis sets based on Karlsruhe def2 sets.[28] Triple-ζ-valence + polarization level basis sets were used for Mn, Ti, La, and O,[29,30] while split-valence + polarization level basis sets were used for Ca and Ba (the Ca basis is included in the ESI†).[31] The Monkhorst–Pack type *k*-meshes for sampling the reciprocal space are listed in the ESI.†[32] Default DFT integration grids and optimization convergence thresholds of CRYSTAL17 were applied in all calculations. The calculations were carried out with the Coulomb and exchange integral tolerance factors (TOLINTEG) set to tight values of 8, 8, 8, 8, and 16. All calculations were carried out with the spin-polarized formalism due to the unpaired electrons of the Mn (II) ions. All reported relative energies are based on electronic energies obtained at 0 K, and Gibbs free energies have not been considered.

CRYSTAL allows the use of the keyword FIXDEF to keep the ratio between two lattice parameters fixed throughout the geometry optimization or to fix a lattice parameter to a certain value. This option was used in some cases where the double perovskite space group arising from both tilting and A-site ordering allowed two lattice parameters to change independently, while the tilt system only would have restricted the two or more tilt angles and pseudocubic lattice parameters to be the same. For example, in the $a^-b^-b^-$ tilt systems, all A-site orderings lead to a monoclinic space group for the double perovskite, while the tilt system alone dictates the pseudocubic *b* and *c* lattice parameters to be the same. The need for the keyword FIXDEF is illustrated by the tilt system $a^-b^-b^-$ with planar A-site ordering (Fig. 3a), which requires the same monoclinic space group $P2/c$ as the tilt system $a^-a^-a^-$ (Fig. 3b). These two systems have initially different lattice parameters, but as they have the same space group without the keyword FIXDEF, a full structural optimization would lead to the same optimized structure. So, FIXDEF was used in this case to constrain the structures to a certain tilt system; however, the energy difference between these two structures with and without the keyword FIXDEF would anyway be very small,

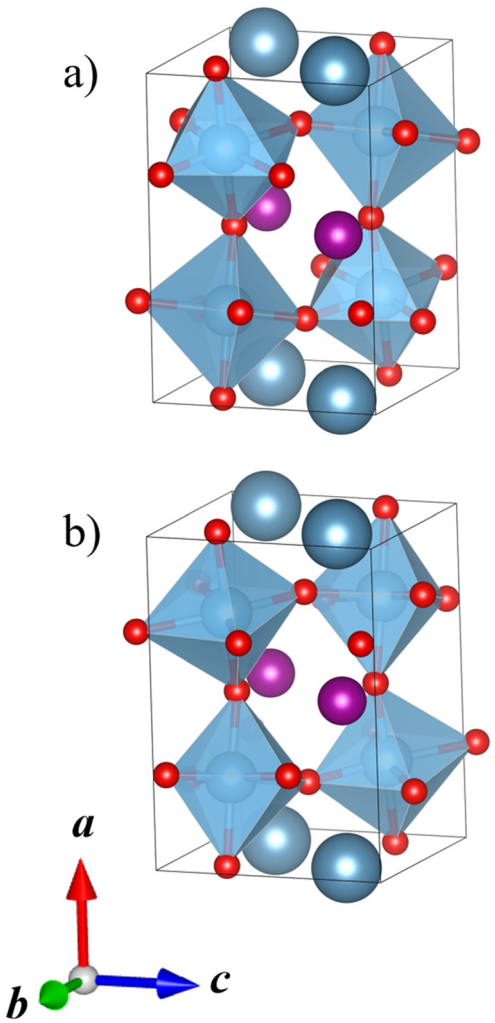

Fig. 3 Two tilt systems of $CaMnTi_2O_6$ with planar A-site ordering (space group $P2/c$): (a) $a^-b^-b^-$ and (b) $a^-a^-a^-$. Ca ions colored in dark grey-blue, Mn ions in purple, Ti ions and their coordination polyhedra in blue, and oxygen anions in red.

clearly less than 1 kJ mol^{-1} per formula unit. Considering the accuracy of the used DFT method, these two tilt systems are thus anyway energetically and practically identical. In the case of rock salt A-site ordering, the tilt systems $a^-b^-b^-$ and $a^-a^-a^-$ could not be fully optimized with the default optimization convergence criteria in CRYSTAL and slightly looser criteria were applied (two to three times larger thresholds). This had no significant impact on the relative energies reported here.

3 Results and discussion

Table 2 shows an overview of the tilt systems and A-site orderings studied for $CaMnTi_2O_6$, together with relative energies obtained with the DFT-PBE0 method. The ESI† also includes the absolute electronic energies of the studied systems and their optimized geometries in CIF format. The $CaMnTi_2O_6$ structure, in the experimentally observed $P4_2mc$ space group,

Table 2 Summary of the relative energies E_{rel} for different tilt systems and A-site ordering of $CaMnTi_2O_6$. The relative energies are given per formula unit (Z). The first row shows the experimental crystal structure of $CaMnTi_2O_6$ optimized with the same DFT-PBE0 method. The Glazer space group is the space group of the tilt system and the double perovskite space group is the space group arising after A-site ordering applied for the tilt system. In those cases where two double perovskite space groups are given, the second space group is the magnetic space group used for calculations with antiferromagnetic ordering of Mn atoms. Examples column lists few A-site ordered double perovskite materials that crystallize in the crystal structures studied in this work

Tilt system	Glazer space group	Double perovskite space group	Examples	E_{rel} [kJ mol^{-1}]
$a^+a^+c^-$		105 $P4_2mc$	$CaMnTi_2O_6$	0
Columnar A-site ordering				
$a^+a^+a^+$	204 $Im\bar{3}$	71 $Immm$		31
$a^+a^+c^-$	137 $P4_2/nmc$	137 $P4_2/nmc$	$CaFeTi_2O_6$	9
$a^-b^+a^-$	62 $Pnma$	11 $P2_1/m$		21
$a^-b^-b^-$	15 $C2/c$	13 $P2/c$		52
$a^-a^-a^-$	167 $R\bar{3}c$	13 $P2/c$		52
$a^0b^+b^+$	139 $I4/mmm$	139 $I4/mmm$/139 $I4/mmm$		44
$a^+b^0c^-$	63 $Cmcm$	25 $Pmm2$		20
$a^0b^-b^-$	74 $Imma$	51 $Pmma$		55
$a^0a^0c^+$	127 $P4/mbm$	65 $Cmmm$		91
$a^0a^0c^-$	140 $I4/mcm$	132 $P4_2/mcm$/111 $P\bar{4}2m$		87
$a^0a^0a^0$	221 $Pm\bar{3}m$	123 $P4/mmm$		184
Planar A-site ordering				
$a^+a^+a^+$	204 $Im\bar{3}$	47 $Pmmm$		65
$a^+a^+c^-$	137 $P4_2/nmc$	115 $P\bar{4}m2$		49
$a^-b^+a^-$	62 $Pnma$	26 $Pmc2_1$	$NdBaMn_2O_6$	26
$a^-b^-b^-$	15 $C2/c$	13 $P2/c$/3 $P2$		41
$a^-a^-a^-$	167 $R\bar{3}c$	13 $P2/c$		41
$a^0b^+b^+$	139 $I4/mmm$	123 $P4/mmm$		70
$a^+b^0c^-$	63 $Cmcm$	38 $Amm2$		38
$a^0b^-b^-$	74 $Imma$	51 $Pmma$		49
$a^0a^0c^+$	127 $P4/mbm$	65 $Cmmm$/65 $Cmmm$		90
$a^0a^0c^-$	140 $I4/mcm$	125 $P4/nbm$/111 $P\bar{4}2m$		82
$a^0a^0a^0$	221 $Pm\bar{3}m$	123 $P4/mmm$	$LaBaMn_2O_6$	183
Rock salt A-site ordering				
$a^+a^+a^+$	204 $Im\bar{3}$	200 $Pm\bar{3}$		63
$a^+a^+c^-$	137 $P4_2/nmc$	115 $P\bar{4}m2$		46
$a^-b^+a^-$	62 $Pnma$	31 $Pmn2_1$		26
$a^-b^-b^-$	15 $C2/c$	5 $C2/3$ $P2$		41
$a^-a^-a^-$	167 $R\bar{3}c$	5 $C2/3$ $P2$		46
$a^0b^+b^+$	139 $I4/mmm$	123 $P4/mmm$/123 $P4/mmm$		63
$a^+b^0c^-$	63 $Cmcm$	38 $Amm2$		35
$a^0b^-b^-$	74 $Imma$	44 $Imm2$		41
$a^0a^0c^+$	127 $P4/mbm$	136 $P4_2/mnm$		78
$a^0a^0c^-$	140 $I4/mcm$	121 $I\bar{4}_2m$		71
$a^0a^0a^0$	221 $Pm\bar{3}m$	225 $Fm\bar{3}m$	$NaBaLiNiF_6$	183

optimized by the same DFT-PBE0 method, was used as a reference (E_{rel} = 0 kJ mol^{-1}). In addition to the octahedral tilting and A-site ordering considered here, the experimental crystal structure in the polar space group $P4_2mc$ shows further energy-lowering atomic displacements that are discussed in detail below. Concerning geometries, the DFT-PBE0 method performs very well when the experimental (300 K) lattice parameters of $CaMnTi_2O_6$ ($P4_2mc$) are compared with DFT-optimized (0 K) lattice parameters: a parameter is underestimated by −0.5% and c-parameter is overestimated by 1.0%.

In the case of columnar A-site ordering, the correct final geometry $a^+b^0c^-$ tilt system could not be obtained. This combination of the tilt system and A-site ordering leads to a relatively low-symmetry space group, $Pmm2$, where the octahedra had the freedom to tilt in a different and more complex way compared to the ideal $a^+b^0c^-$ tilting. Here, we report the relative energy for the fully optimized structure which cannot be described by the Glazer notation, as this resulted in a relatively low-energy geometry with (E_{rel} = 20 kJ mol^{-1}) that is the second-lowest in energy after columnar A-site ordering with $a^+a^+c^-$ tilting (E_{rel} = 9 kJ mol^{-1}). This is also an example of a situation where a full DFT treatment may reveal structural alternatives that cannot be predicted simply by considering idealized tilt systems with empirical rules. However, the ideal tilt systems still provide the best starting point for a systematic study of the various structural alternatives.

The energy differences between the calculated A-site ordering/tilt system combinations and the experimental $CaMnTi_2O_6$ structure range from 9 kJ mol^{-1} to 184 kJ mol^{-1} per formula unit (Table 2). In all three orderings, the ideal perovskite structure, $a^0a^0a^0$, has by far the highest energy difference of over 180 kJ mol^{-1} per formula unit. The non-tilted highest-energy structures are followed by the single tilt systems, $a^0a^0c^+$ and $a^0a^0c^-$. The energy differences between two- and three-tilt systems are already much smaller and both options can lead to low-energy structures. Two tilts such as $a^0b^-b^-$ already

decreased the energy difference immensely compared to the untilted ideal perovskite structure, down to, for example, 41 kJ mol^{-1} in the rock salt ordering.

Table 2 shows that in the planar and rock salt ordering, the $a^-b^+a^-$-tilts are the lowest energy ones and even in the columnar ordering, it is the second-lowest one if the $a^+b^0c^-$-tilt is not taken into account (optimization in the low-symmetry space group led to a tilt system that cannot be described by the Glazer notation). Generally, the energy ordering of tilt systems clearly varies within all three A-site orderings. When we looked for correlations between the relative energy and the lattice parameters or the relative energy and the Ti–O distances, we did not find any. Since the tilt angles are related to the lattice parameters, they also did not show any reasonable correlation with the relative energies. Therefore, we looked into A-site cations to find correlations between the structural parameters and the relative energies of the studied systems.

The A-site cations play a major role in the tilting of octahedra in perovskites. Therefore, it is likely that the A-site cations are also a major driving force for the relative energy differences obtained for the different tilt systems. In particular, the coordination number and bond lengths of A atoms with the surrounding oxygen atoms play a key role. While in the specific case of $CaMnTi_2O_6$ the Ca–O interactions are strongly ionic (Pauling electronegativity difference 2.44), the Mn–O bonds may possess slightly more covalent nature (Pauling electronegativity difference 1.89). This leads to the coordination of Mn ions being the main driving force in $CaMnTi_2O_6$ for the relative energy differences. Even though a six-fold coordination is common for Mn^{2+}, the preferred coordination of Mn in $CaMnTi_2O_6$ is four: in the experimental $CaMnTi_2O_6$ crystal structure, half of the Mn cations are square-planar coordinated and half of them tetrahedrally coordinated. Of the tilt systems studied here, the only tilt system that allows Mn to be six-fold coordinated is $a^+b^0c^-$. The resulting coordination polyhedron can be considered as a distorted trigonal prism and this coordination for Mn is not energetically favorable.

Fig. 4 shows the distance between Mn and O atoms for all 11 tilt systems and also the sum of the ionic radii of Mn(II) and O(-II) as a reference point for an "ideal" Mn–O distance.[33] For each A-site ordering, the x-axis in the plot lists the tilt systems from the lowest (left) to the highest (right) relative energy with respect to the optimised $CaMnTi_2O_6$ structure, in the experimentally observed $P4_2mc$ space group. Different coordination numbers are also denoted in addition to the Mn–O distances.

The distances between Mn and O atoms range from 2.09 Å in the planar $a^0b^+b^+$ system to 2.72 Å in the columnar and planar $a^0a^0a^0$ systems. For all three high-energy $a^0a^0a^0$ systems, the Mn–O distances are way too long for any covalent interaction. Overall, there is a tendency for higher-energy tilt systems to have longer Mn–O distances. However, there are also exceptions. For example, in columnar A-site ordering, the tilt system $a^0b^+b^+$ has square-planar coordinated Mn cations with Mn–O distances close to the sum of the ionic radii and hence rather optimal bond lengths, but still the tilt system is not among the lowest-energy ones. The reason for this is that

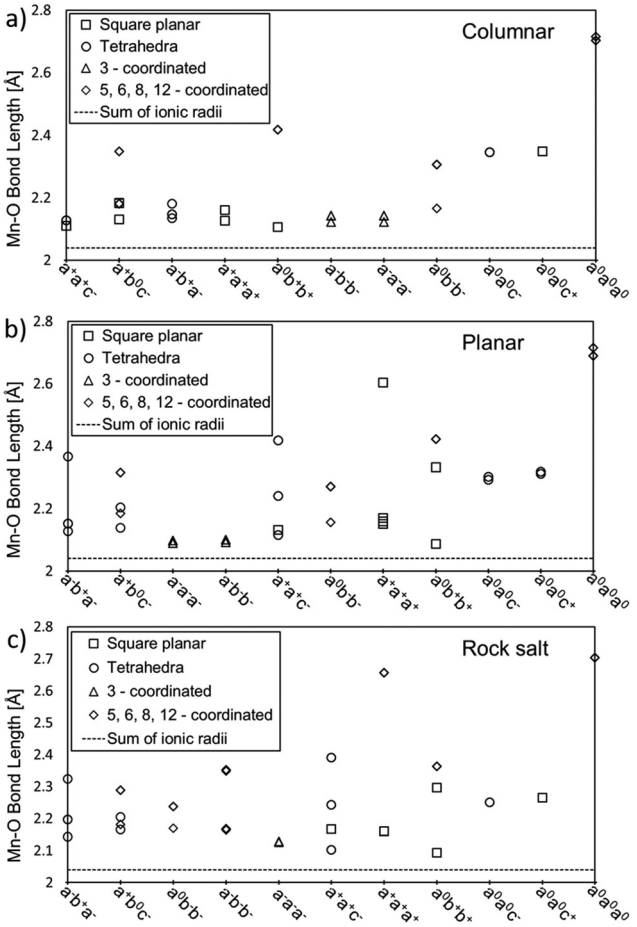

Fig. 4 Mn–O distances for all studied tilt systems and A-site ordering: (a) columnar, (b) planar, and (c) rock salt. The x-axis lists the tilt systems from the lowest (left) to the highest (right) relative energy with respect to the experimental $CaMnTi_2O_6$ structure. Different coordinations are depicted by squares for square planar coordination, circles for tetrahedral coordination, triangles for three-fold coordination and diamonds for more than four-fold coordination. The sum of ionic radii of Mn(II) (0.66 Å) and O(-II) (1.38 Å) is shown by a dotted line at the bottom of each plot.[33]

there are also Mn ions which are 8-coordinated with a long Mn–O distance of about 2.4 Å.

In the case of planar A-site ordering, the Mn–O distances in $a^-a^-a^-$ and $a^-b^-b^-$ are rather short and even closer to the sum of ionic radii than in the lowest-energy tilt system $a^-b^+a^-$, but the coordination of the Mn atoms is 3-fold and not the optimal 4-fold. Another good example of the planar A-site ordering is the high-energy $a^+a^+a^+$ tilt system where all Mn atoms have square-planar coordination and most Mn–O distances are rather close to the ideal sum of ionic radii. However, there is one Mn–O distance of about 2.6 Å, which drives the energy of this tilt system up.

In a similar fashion to the rock salt A-site ordering, the $a^0b^+b^+$ tilt system has the shortest Mn–O distance of about 2.1 Å in square planar coordination but is still far from the lowest energy tilt system in energy. The reason is that this tilt

system also contains 8-coordinated manganese cations with a long Mn–O distance of about 2.4 Å. A particularly interesting case in the rock salt A-site ordering is the tilt system $a^0a^0c^+$. In principle, the Mn atoms have optimal square-planar coordination and the Mn–O distances are not excessively long, but still this tilt system has the second-highest relative energy. In this case, other structural factors may also play a role: there are Ca–O distances of 2.27 Å, which are significantly shorter compared to typical Ca–O distances.

Comparing the lowest-energy tilt systems of planar and rock salt A-site ordering ($a^-b^+a^-$ in both cases) with the lowest energy tilt system in columnar ordering ($a^+a^+c^-$), it is clear that the difference in energy here seems to originate from the different Mn–O distances. While in all three A-site orderings the lowest-energy tilt systems contain only 4-coordinated Mn cations, in planar and rock salt ordering some of the bond lengths range between 2.3 Å and 2.4 Å, whereas in columnar ordering all Mn–O distances are about 2.1 Å long and close to the sum of the ionic radii.

Our DFT calculations correctly predict that the lowest-energy combination of A-site ordering and tilt systems is the columnar-ordered $a^+a^+c^-$ tilt system (Fig. 5a) that has been found in the experimental crystal structure of $CaMnTi_2O_6$ (Fig. 5b).[21] However, even though the experimental and computational A-site ordering and the tilt system are in agreement, the optimised $CaMnTi_2O_6$ structure in the experimentally observed $P4_2mc$ space group is 9 kJ mol^{-1} lower in energy compared to the lowest-energy calculated structure. This non-negligible difference arises from the atomic displacement of the square-planar Mn ions, together with the slight displacement of Ti ions, discussed in detail by Gou *et al.*[19] In the experimental structure, the Mn cations are displaced slightly out of the square plane and the symmetry is decreased from the non-polar space group $P4_2/nmc$ to the polar space group $P4_2mc$. In our screening of the A-site ordering and tilt systems, we used the non-polar $CaFeTi_2O_6$ crystal structure ($P4_2/nmc$) as a starting point for the columnar $a^+a^+c^-$ tilt system. In this structure, the square-planar Mn ions stay in the square plane and Ti ions stay in the center of the octahedra. If the symmetry of the structure is lowered to $P4_2mc$ and the Mn atoms are allowed to be displaced from the square plane, the energy is further lowered.

In this work, we have focused on the A-site ordering and tilting of the octahedra and have not systematically studied the effect of atomic displacements such as ferroelectric distortion. Group-theoretical analyses of octahedral tilting in ferroelectric perovskites have been carried out, showing that the number of structural alternatives increases significantly even for simple perovskites.[34,35] For double perovskites, the A- or B-site ordering further has to be taken into account. A systematic DFT study of such ferroelectric distortion in A-site ordered perovskites is expected to provide similar insights into their structural principles and energetics as the present investigation. In the case of $CaMnTi_2O_6$, the energetic effect of the ferroelectric displacements is 9 kJ mol^{-1} per formula unit, which is still less than the energy difference between the lowest energy and second lowest energy tilt systems studied in this work (11 kJ mol^{-1} per formula unit). Therefore, already the study of A-site ordering and tilting of octahedra seems to provide reasonable and useful structural predictions even for ferroelectric double perovskites.

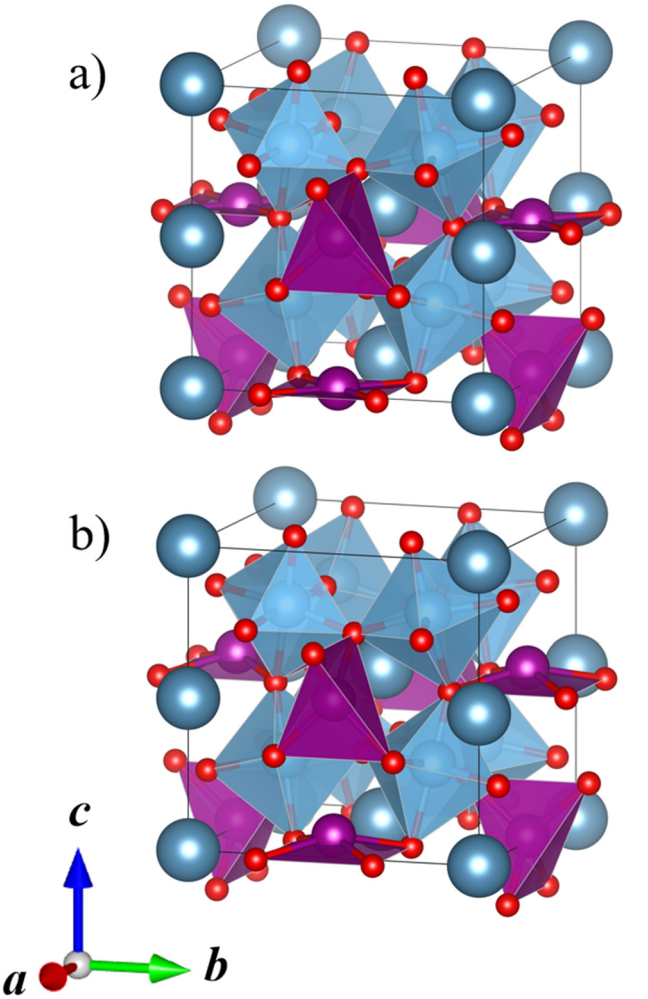

Fig. 5 (a) Calculated lowest-energy structure of $CaMnTi_2O_6$ ($P4_2/nmc$, E_{rel} = 9 kJ mol^{-1} per formula unit). (b) Experimental ferroelectric $CaMnTi_2O_6$ structure with the square-planar Mn cations displaced ($P4_2mc$, E_{rel} = 0 kJ mol^{-1} per formula unit).[21] Ca ions colored in dark grey-blue, Mn ions in purple, Ti ions and their coordination polyhedra in blue, and oxygen anions in red.

We also benchmarked our computational approach for $LaBaMn_2O_6$, which is an A-site ordered double perovskite crystallizing in the space group $P4/mmm$ ($a^0a^0a^0$ tilt system, planar A-site ordering).[36] Four structural alternatives were calculated, mainly to study the energetic effect of the A-site ordering (Table 3). In our calculations, the experimentally found combination of the tilt system and A-site ordering comes out as the lowest energy one. The columnar A-site ordering is only 3 kJ mol^{-1} per formula unit higher in energy, while the rock salt ordering already has a clear difference from the planar ordering. In this double perovskite, La and Ba cations do not

Table 3 Relative energies E_{rel} per formula unit of the A-site ordered $LaBaMn_2O_6$ double perovskite in four different structural models. The $a^0a^0a^0$ tilt system with planar A-site ordering is the one that has been observed experimentally and the one that also has the lowest relative energy here. $LaBaMn_2O_6$ calculated in the experimental structure of $CaMnTi_2O_6$ is also included as a point of comparison

Structure	Tilt system	Space group	E_{rel} [kJ mol^{-1}]
Planar $LaBaMn_2O_6$ (exp.)	$a^0a^0a^0$	$P4/mmm$	0
Columnar $LaBaMn_2O_6$	$a^0a^0a^0$	$P4/mmm$	3
Rock salt $LaBaMn_2O_6$	$a^0a^0a^0$	$P4/mmm$	30
$CaMnTi_2O_6$ (exp.)	$a^+a^+c^-$	$P4_2mc$	6

provoke tilting of the octahedra and the non-tilted ideal structure is less prone to the influence of the A-site ordering (planar *vs.* columnar). When $LaBaMn_2O_6$ is optimized in the experimental $CaMnTi_2O_6$ crystal structure with tilted octahedra ($P4_2mc$), the structure is higher in energy compared to the non-tilted structure. However, the energy difference is only 6 kJ mol^{-1} per formula unit.

4 Conclusions

We have used quantum chemical methods to study systematically all relevant combinations of cation ordering and tilting in A-site ordered $AA'B_2O_6$ double perovskites. The used DFT-PBE0 method is able to predict the correct combination of A-site ordering and tilting of octahedra in comparison to the experimentally known $CaMnTi_2O_6$ double perovskite. The energy differences between the various combinations of A-site ordering and tilt systems show a large variation of tens of kJ mol^{-1} per formula unit, which suggests that the methodology used here can be used as a starting point for making reliable predictions on the structures of yet unknown A-site ordered double perovskites. The energy differences due to A-site ordering and octahedral tilting were larger compared to the energy difference arising from ferroelectric distortion in $CaMnTi_2O_6$. We investigated the relative energies of various $CaMnTi_2O_6$ structural alternatives in detail and the main driving forces for the energy differences are Mn–O distances and Mn coordination. Similar structural analysis can be readily extended to A-site ordered double perovskites with other compositions. The methodology used here can be further improved and extended to several directions. Consideration of phonon properties and thermodynamics (Gibbs free energies) would further improve the accuracy of the predictions. To enable full investigation of thermodynamics, the computational efficiency probably needs to be increased by using for example semi-empirical tight-binding density functional methods,[37] but benchmarking with respect to standard DFT methods is needed first. The methodology can be extended towards ferroelectric distortion with the help of previous group-theoretical groundwork.[34,35] Finally, a similar approach can also be used to make predictions for B-site ordered double perovskites, where group-theoretical groundwork has also been laid,[34,35] but magnetism will play a more significant role compared to the work presented here.

Author contributions

Elisabeth K. Albrecht: Conceptualization, investigation, visualization, writing – original draft preparation, and writing – review and editing. Antti. J. Karttunen: Conceptualization, writing – review and editing, supervision, and funding acquisition. All authors have read and agreed to the published version of the manuscript.

Conflicts of interest

There are no conflicts to declare.

Acknowledgements

We thank the Academy of Finland for funding (Grant No. 317273) and CSC – The Finnish IT Center for Science for computational resources.

References

1 R. J. D. Tilley, *Perovskites: structure-property relationships*, Wiley, Chichester, West Sussex, United Kingdom, 1st edn, 2016.
2 N. Xie, J. Zhang, S. Raza, N. Zhang, X. Chen and D. Wang, *J. Phys.: Condens. Matter*, 2020, **32**, 315901.
3 H. W. Eng, P. W. Barnes, B. M. Auer and P. M. Woodward, *J. Solid State Chem.*, 2003, **175**, 94–109.
4 M. W. Lufaso and P. M. Woodward, *Acta Crystallogr., Sect. B: Struct. Sci.*, 2004, **60**, 10–20.
5 A. M. Glazer, *Acta Crystallogr., Sect. B: Struct. Crystallogr. Cryst. Chem.*, 1972, **28**, 3384–3392.
6 P. M. Woodward, *Acta Crystallogr., Sect. B: Struct. Sci.*, 1997, **53**, 44–66.
7 P. M. Woodward, *Acta Crystallogr., Sect. B: Struct. Sci.*, 1997, **53**, 32–43.
8 K. Momma and F. Izumi, *J. Appl. Crystallogr.*, 2011, **44**, 1272–1276.
9 G. King and P. M. Woodward, *J. Mater. Chem.*, 2010, **20**, 5785.
10 M. C. Knapp and P. M. Woodward, *J. Solid State Chem.*, 2006, **179**, 1076–1085.
11 P. Davies, H. Wu, A. Borisevich, I. Molodetsky and L. Farber, *Annu. Rev. Mater. Res.*, 2008, **38**, 369–401.
12 A. A. Belik, *Dalton Trans.*, 2018, **47**, 3209–3217.
13 S. Vasala and M. Karppinen, *Prog. Solid State Chem.*, 2015, **43**, 1–36.
14 V. M. Goldschmidt, *Naturwissenschaften*, 1926, **14**, 477–485.
15 M. R. Filip and F. Giustino, *Proc. Natl. Acad. Sci. U. S. A.*, 2018, **115**, 5397–5402.

16 C. J. Bartel, C. Sutton, B. R. Goldsmith, R. Ouyang, C. B. Musgrave, L. M. Ghiringhelli and M. Scheffler, *Sci. Adv.*, 2019, **5**, eaav0693.
17 F. Shojaei and W.-J. Yin, *J. Phys. Chem. C*, 2018, **122**, 15214–15219.
18 J. Ding, Y. Liu and Y. Zhang, *J. Magn. Magn. Mater.*, 2021, **535**, 168035.
19 G. Gou, N. Charles, J. Shi and J. M. Rondinelli, *Inorg. Chem.*, 2017, **56**, 11854–11861.
20 J. Herrero-Martín, J. Ruiz-Fuertes, T. Bernert, M. Koch-Müller, E. Haussühl and J. L. García-Muñoz, *Phys. Rev. B*, 2018, **97**, 235129.
21 A. Aimi, D. Mori, K.-i. Hiraki, T. Takahashi, Y. J. Shan, Y. Shirako, J. Zhou and Y. Inaguma, *Chem. Mater.*, 2014, **26**, 2601–2608.
22 Z. Li, Y. Cho, X. Li, X. Li, A. Aimi, Y. Inaguma, J. A. Alonso, M. T. Fernandez-Diaz, J. Yan, M. C. Downer, G. Henkelman, J. B. Goodenough and J. Zhou, *J. Am. Chem. Soc.*, 2018, **140**, 2214–2220.
23 C. J. Howard and H. T. Stokes, *Acta Crystallogr., Sect. B: Struct. Sci.*, 1998, **54**, 782–789.
24 M. W. Lufaso and P. M. Woodward, *Acta Crystallogr., Sect. B: Struct. Sci.*, 2001, **57**, 725–738.
25 R. Dovesi, A. Erba, R. Orlando, C. M. Zicovich-Wilson, B. Civalleri, L. Maschio, M. Rérat, S. Casassa, J. Baima, S. Salustro and B. Kirtman, *Wiley Interdiscip. Rev.: Comput. Mol. Sci.*, 2018, **8**, 1–36.
26 J. P. Perdew, K. Burke and M. Ernzerhof, *Phys. Rev. Lett.*, 1996, **77**, 3865–3868.
27 C. Adamo and V. Barone, *J. Chem. Phys.*, 1999, **110**, 6158–6170.
28 F. Weigend and R. Ahlrichs, *Phys. Chem. Chem. Phys.*, 2005, **7**, 3297.
29 M. S. Kuklin, K. Eklund, J. Linnera, A. Ropponen, N. Tolvanen and A. J. Karttunen, *Molecules*, 2022, **27**, 1–26.
30 A. J. Karttunen, T. Tynell and M. Karppinen, *Nano Energy*, 2016, **22**, 338–348.
31 S. I. Ivlev, A. J. Karttunen, M. R. Buchner, M. Conrad, R. V. Ostvald and F. Kraus, *Crystals*, 2018, **8**, 1–14.
32 H. J. Monkhorst and J. D. Pack, *Phys. Rev. B: Solid State*, 1976, **13**, 5188–5192.
33 R. D. Shannon, *Acta Crystallogr., Sect. A: Cryst. Phys., Diffr., Theor. Gen. Crystallogr.*, 1976, **32**, 751–767.
34 H. T. Stokes, E. H. Kisi, D. M. Hatch and C. J. Howard, *Acta Crystallogr., Sect. B: Struct. Sci.*, 2002, **58**, 934–938.
35 K. S. Aleksandrov and J. Bartolomé, *Phase Transitions*, 2001, **74**, 255–335.
36 T. Nakajima, H. Kageyama, H. Yoshizawa, K. Ohoyama and Y. Ueda, *J. Phys. Soc. Jpn.*, 2003, **72**, 3237–3242.
37 C. Bannwarth, E. Caldeweyher, S. Ehlert, A. Hansen, P. Pracht, J. Seibert, S. Spicher and S. Grimme, *Wiley Interdiscip. Rev.: Comput. Mol. Sci.*, 2021, **11**, e1493.